AIP | Applied Physics Letters

Light absorption enhancement of ~100 nm thick poly(3-hexylthiophene) thin-film by embedding silver nanoparticles

Yinghui Cao, Peng Du, Yanfeng Qiao, Zhenyu Liu, and Zaicheng Sun

Citation: Applied Physics Letters **105**, 153902 (2014); doi: 10.1063/1.4898600
View online: http://dx.doi.org/10.1063/1.4898600
View Table of Contents: http://scitation.aip.org/content/aip/journal/apl/105/15?ver=pdfcov
Published by the AIP Publishing

Light absorption enhancement of ~100 nm thick poly(3-hexylthiophene) thin-film by embedding silver nanoparticles

Yinghui Cao,[1,2,a)] Peng Du,[3,4,a)] Yanfeng Qiao,[1] Zhenyu Liu,[1,b)] and Zaicheng Sun[3]
[1]*Changchun Institute of Optics, Fine Mechanics and Physics, 3888 East Nanhu Road, Changchun, Jilin 130033, People's Republic of China*
[2]*College of Computer Science and Technology, Jilin University, 2699 Qianjin Street, Changchun, Jilin 130021, People's Republic of China*
[3]*State Key Laboratory of Luminescence and Applications, Changchun Institute of Optics, Fine Mechanics and Physics, 3888 East Nanhu Road, Changchun, Jilin 130033, People's Republic of China*
[4]*Graduate University of Chinese Academy of Science, 19A Yuquanlu, Beijing 100049, People's Republic of China*

(Received 4 September 2014; accepted 7 October 2014; published online 16 October 2014)

In this work, we experimentally and numerically investigate the field enhancement and light absorption enhancement in poly(3-hexylthiophene) (P3HT) thin-film by embedding silver nanoparticles (Ag NPs). Experimental results show that light absorption of ~100 nm thick P3HT thin-film is enhanced by embedding Ag NPs of diameter 20 ~ 50 nm in the film. Numerical simulations show that by embedding coupled silver nanospheres (Ag NSs) of diameter 20–40 nm into P3HT, the region of field enhancement can be extended about 100 nm towards the incident light source, due to the interference between the incident field and the scattered field of the coupled Ag NSs. The long-distance field enhancement effect of large-sized Ag NPs can be used to improve the efficiency of organic thin-film solar cell devices. © *2014 AIP Publishing LLC*.
[http://dx.doi.org/10.1063/1.4898600]

Organic solar cell devices have attracted great interests for having advantages such as low-cost, light-weight, low temperature fabrication, and solution-based process.[1–3] In recent years, for high-performance organic solar cell devices, the power conversion efficiency already exceeds 11%.[4] However, because of the low charge-carrier mobility and short exciton diffusion length, the thickness of organic photoactive layer is limited to within a few hundreds nanometers, and leads to low light absorption of the organic solar cell devices.[5,6]

One of the effective method of improving light absorption of organic solar cell is to exploit the surface plasmonic effects of noble metal nanoparticles.[7] Silver nanoparticles (Ag NPs) have intensive Local Surface Plasmon Resonance (LSPR) effects[8–13] in visible light region, and were extensively employed for light absorption enhancement by introducing the nanoparticles into the solar cell devices.[14–19] One of the LSPR effects is the local field enhancement effect, in which case light is concentrated around the metal nanoparticles, thus the field intensity in the vicinity of the nanoparticles, as well as, the light absorption in surrounding photoactive material are increased. However, as the surface plasmons (SPs) are collective excitations of electrons near the metal surfaces,[9,10,12] the local field enhancement are localized to the surfaces of nanoparticles.

In this work, we experimentally measure the light absorption enhancement of poly(3-hexylthiophene) (P3HT) thin-film samples, which are embedded with Ag NPs of 20–50 nm in diameter, and analyse the relation between the light absorption enhancement and the film thickness. In addition, we use numerical simulations to investigate the mechanism and conditions of field enhancement and light absorption enhancement in P3HT at long distances from the embedded Ag NPs.

In our experiments, Ag NPs are synthesized following the procedure reported by Silvert *et al.*[20] A scanning electron microscope (SEM) image of the synthesized Ag NPs is shown in Fig. 1(a), which is obtained from a JEOL JSM 4800F scanning electron microscope. P3HT thin-films are prepared by spin-coating Ag NPs and P3HT on the glass substrates successively; a schematic diagram of the film structure is shown in Fig. 1(b). The spin-coating time is set as 1 min, with the spin speed of 700 rpm. By changing the concentration of P3HT in chlorobenzene, P3HT thin-film samples with thickness of 32, 58, and 103 nm are prepared, respectively. The film thickness are measured using a Veeco Dekatak 150 surface profiler. Samples of the pristine P3HT thin-film alone are also prepared, serving as a reference in measuring absorption enhancement.

The light absorption of the samples are measured using the Shimadzu UV-3101 spectrophotometer. The absorption spectra of the 103-nm-thick P3HT thin-film embedded with Ag NPs, and the pristine P3HT thin-film without Ag NPs are shown in Fig. 1(c), indicated by the symbol A and A_{ref}, respectively. In Fig. 1(c), we observe that light is strongly absorbed by P3HT in the spectra range of 400–650 nm, with two distinct vibronic peaks at 520 and 560 nm, respectively. The absorption enhancement ΔA is calculated as $\Delta A = A - A_{ref}$, as shown in Fig. 1(c). For the 103-nm-thick P3HT thin-film sample, both the absorption A and the absorption enhancement ΔA reach their maximum between the two vibronic peaks.

The absorption enhancement ΔA of the P3HT thin-film samples with different thickness are shown in Fig. 1(d),

[a)]Y. Cao and P. Du contributed equally to this work
[b)]liuzy@ciomp.ac.cn

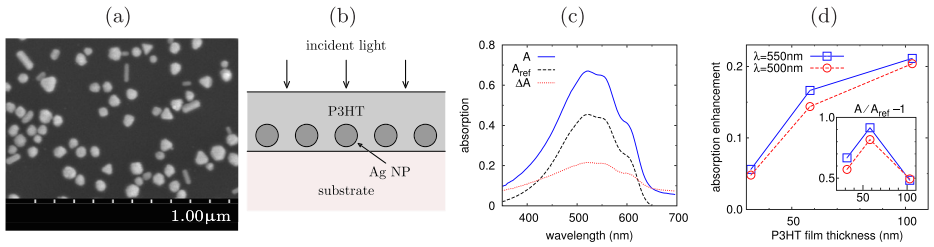

FIG. 1. (a) A SEM image of the synthesized Ag NPs. (b) Structure of the experimental samples of P3HT film, embedded with Ag NPs. (c) Absorption spectra of the 103-nm-thick P3HT thin-film samples. (d) The absorption enhancement of the P3HT thin-film samples. An inset in the figure shows the relative absorption enhancement of the samples.

which are calculated at the wavelength of 500 and 550 nm, respectively. An inset in Fig. 1(d) shows the relative absorption enhancements of the samples, which are calculated by $\Delta A/A_{ref} = A/A_{ref} - 1$. In Fig. 1(d), we observe that when the film thickness changes from 32 to 58 nm, the absorption enhancement ΔA increases rapidly, which implies that in the vicinity of the embedded Ag NPs, the local field enhancement contributes substantially to the absorption enhancement. When the film thickness changes form 58 to 103 nm, the absorption enhancement increases slowly, which implies that at long distances, the field enhancement is weaker than that in the vicinity of the embedded Ag NPs, but still contributes to the absorption enhancement.

In a previous work, Rand reported that by embedding approximately 5-nm-diameter Ag NPs, the light absorption enhancement of surrounding organic photoactive material is confined to about 10 nm around the embedded Ag NPs.[15] However, in this work experimental results show that light absorption of 103-nm-thick P3HT thin-film is enhanced by embedding Ag NPs of 20–50 nm in the film, indicating that field in the 103-nm-thick P3HT film is enhanced by the embedded Ag NPs. In the following paragraphs, we will use numerical simulations to investigate the mechanism and conditions of the field enhancement at long-distances from the embedded Ag NPs.

In this work, we use commercial finite element software package COMSOL to simulate Ag NPs and calculate their light absorption enhancement effects and field enhancement effects. The permittivity data of silver and organic photoactive material P3HT are taken from the optical constant book by Palik,[21] and the work of Monistier,[22] respectively. As a simple model of the dispersed Ag NPs, arrays of silver nanospheres (Ag NSs), with Ag NS diameter of $d = 20$, 30, and 40 nm, and inter-particle distance of $s = 0.5d$, d, $1.5d$, are simulated, respectively. The Ag NSs array lies in the xy plane, surrounded by P3HT, as shown in Fig. 2(a). The incident electric field propagates along the negative z axis, with polarization along the x axis. The electric field can be calculated by solving electromagnetic wave equation, some figures of the calculated field are shown in the supplementary material.[23]

After solving the electric field, the field enhancement can be calculated as the ratio of the total field to the incident field $|\mathbf{E}|/|\mathbf{E}_{inc}|$. For the 30-nm-diameter Ag NSs array, with inter-particle distance of 15 nm, the field enhancement in xz plane is shown in Fig. 2(b). The field enhancement is calculated at the wavelength of 500 nm. In Fig. 2(b), we observe that the field enhancement is quite low, even at the "hot spot" the field intensity is below 10 times of the incident field. This can be explained as the suppression of the surface plasmonic effects of the embedded Ag NPs by the surrounding light absorbing medium.[15,17] In addition, we can see that besides the local field enhancement in the vicinity of the embedded Ag NSs, the field is weakly enhanced in the region $30\,\text{nm} < z < 100\,\text{nm}$, with field enhancement factor of 1–1.16 for the 30-nm-diameter Ag NSs array. Although the field enhancement is weak in this region, it still can contribute to the light absorption enhancement of surrounding P3HT because of its comparatively large size, as discussed in the next paragraph. The weakly enhanced field in this region explains the experimental observation that the absorption enhancement of P3HT thin-

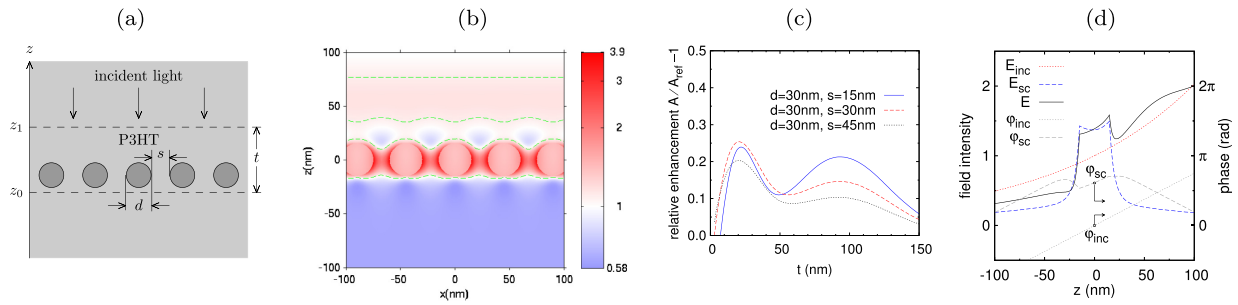

FIG. 2. (a) Schematic diagram for the simulation of Ag NSs array, with Ag NSs diameter d and inter-particle distance s. (b) The field enhancement ($|\mathbf{E}|/|\mathbf{E}_{inc}|$) for Ag NSs array of $d = 30$ nm, $s = 15$ nm, in xz plane. To emphasize the small variations of field enhancement and field weakening, logarithmic scale color map is used, in which the red color represents the field enhancement, and the blue color represents the field weakening. The dashed line (in green) indicates the contour line of field enhancement factor 1.1. (c) The relative absorption enhancement of Ag NSs array, with Ag NSs diameter $d = 30$ nm, and inter-particle distance $s = 15$, 30, and 45 nm. (d) The electric field components of the Ag NSs array, with $d = 30$ nm and $s = 15$ nm, along z axis. The symbols E_{inc}, E_{sc}, E refer to the intensity of the incident field, the scattered field, and the total field, respectively. The symbols φ_{inc} and φ_{sc} refer to the phase of the incident field and the scattered field, respectively.

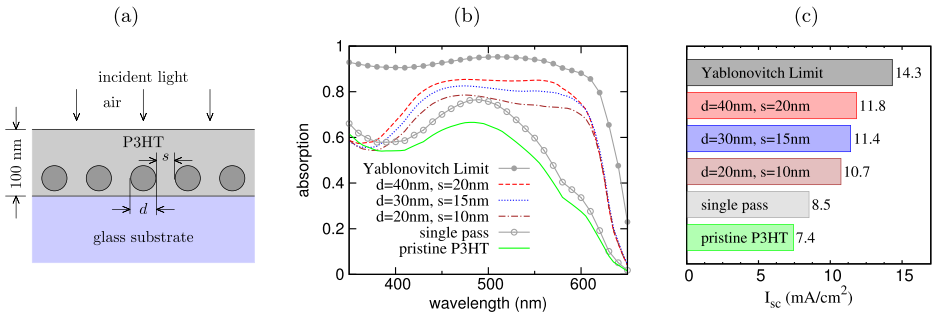

FIG. 3. (a) Schematic diagram of the P3HT thin-film model, for the calculation of the absorption spectra and the photocurrent. (b) The absorption spectra of the simulated P3HT thin-film, with embedded Ag NSs of diameter $d = 20$, 30, and 40 nm, and inter-particle distance $s = d/2$. The absorption spectrum of the simulated pristine P3HT thin-film, and the spectrum of the single pass absorption, as well as the spectrum of the Yablonovitch limit are also shown in the figure. (c) The photocurrent of the simulated P3HT thin-film, calculated by integrating over the AM 1.5 solar spectrum.

film embedded with Ag NPs increases slowly when the film thickness changes from 58 to 103 nm.

In order to calculate the absorption enhancement, we define the symbol $A(t)$ as the light absorption of the P3HT layer of thickness t, which lies between $z_0 \le z \le z_1$, enclosing the embedded Ag NSs but excluding the volume of the Ag NSs, as shown in Fig. 2(a). z_0 is 2 nm below the embedding Ag NSs, and $z_1 = z_0 + t$. Similarly, we define a reference absorption $A_{ref}(t)$ of the pristine P3HT layer, which does not contain the Ag NSs. Then the relative absorption enhancement can be calculated as $A(t)/A_{ref}(t) - 1$. The relative absorption enhancement of the 30-nm-diameter Ag NSs array is shown in Fig. 2(c). For Ag NSs of other sizes, the relative absorption enhancements are shown in the supplementary material.[23] In the figure, the relative absorption enhancements increase rapidly when t is small, and reach their maxima at $t \approx 20$ nm, due to the local field enhancement at the vicinity of Ag NSs. At $t \approx 80$ nm, the relative absorption enhancements reach their second maxima, with relative enhancement factor of 0.1–0.2 ($A \approx 1.1A_{ref} \sim 1.2A_{ref}$), because of field enhancement at long distances from the embedded Ag NSs.

In order to understand the mechanism of the long-distance field enhancement of Ag NPs embedded in P3HT, the electric field components along axis z, of the Ag NSs array with $d = 30$ nm and $s = 15$ nm, are shown in Fig. 2(d). The field components are calculated at the wavelength of 500 nm and plotted along z axis. For Ag NSs of other sizes, the field components are shown in the supplementary material.[23] We observe that in region $z = 30$–100 nm, the phase differences between the incident and the scattered field, which can be written as $\Delta\varphi = \varphi_{inc} - \varphi_{sc}$, are approximately in the range $|\Delta\varphi| \le \pi/2$, thus field is enhanced in this region. On the other hand, field is weakened in region $z < -30$ nm, because of the phase difference $|\Delta\varphi| > \pi/2$ in the region. The long-distance field enhancement and field weakening of Ag NPs result from the constructive and destructive interference between the incident field and the scattered field from Ag NPs.

To evaluate the light absorption of Ag NSs enhanced P3HT thin-film when irradiated by sunlight, we simulate a 100-nm-thick P3HT thin-film, which is embedded with Ag NSs array, and located on glass substrate, as shown in Fig. 3(a). The absorption spectra of the simulated film, with embedded Ag NPs of diameter $d = 20$, 30, and 40 nm, and inter-particle distance $s = d/2$, are shown in Fig. 3(b). As references, the absorption spectrum of the simulated pristine P3HT thin-film, the spectrum of the single pass absorption, as well as the spectrum of the Yablonovitch limit[24] are also calculated and shown in Fig. 3(b). Further, by integrating over the AM 1.5 solar spectrum, the photocurrent of the simulated P3HT thin-film is calculated and shown in Fig. 3(c). From Figs. 3(b) and 3(b), we can see that the light absorption and photocurrent of the 100-nm-thick P3HT thin-film are effectively enhanced by the embedded Ag NSs.

In experiments, we observed that the light absorption of ~100 nm thick P3HT film is enhanced by embedding Ag NPs of diameter 20–50 nm in the film. Numerical simulations show that by embedding coupled Ag NSs of 20–40 nm in diameter into P3HT, the region of field enhancement can be extended ~100 nm towards the incident light source, because of the interference between the incident field and the scattered field of the coupled Ag NSs. This effect can be used to improve the efficiency of organic thin-film solar cell devices.

This work was supported by the National Natural Science Foundation of China (Nos. 51275504, 61306081, and 61176016), Science and Technology Development Plane of JiLin Province (20140519007JH), and Natural Science Foundation of Jilin Province (No. 20130522142JH). Z. Sun gratefully thanks the support of the "Hundred Talent Program" of Chinese Academy of Sciences. Y. Cao gratefully thanks the support of the Startup fund for postdoctoral scientific research program of Jilin Province.

[1]H. Y. Chen, J. H. Hou, S. Q. Zhang, Y. Y. Liang, W. G. Yang, Y. Yang, L. P. Yu, Y. Wu, and G. Li, "Polymer solar cells with enhanced open-circuit voltage and efficiency," Nat. Photonics **3**, 649–653 (2009).
[2]S. H. Park, A. Roy, S. Beaupre, S. Cho, N. Coates, J. S. Moon, D. Moses, M. Leclerc, K. Lee, and A. J. Heeger, "Bulk heterojunction solar cells with internal quantum efficiency approaching 100%," Nat. Photonics **3**, 297–303 (2009).
[3]M. Chang, D. Choi, B. Fu, and E. Reichmanis, "Solvent based hydrogen bonding: impact on poly(3-hexylthiophene) nanoscale morphology and charge transport characteristics," ACS Nano **7**, 5402–5413 (2013).
[4]C. C. Chen, W. H. Chang, K. Yoshimura, K. Ohya, J. You, Z. Hong, and Y. Yang, "An efficient triple-junction polymer solar cell having a power conversion efficient exceeding 11%," Adv. Mater. **26**, 5670–5677 (2014).
[5]P. W. M. Blom, V. D. Mihailetchi, L. J. A. Koster, and D. E. Markov, "Device physics of polymer:fullerene bulk heterojunction solar cells," Adv. Mater. **19**, 1551–1566 (2007).

[6]D. E. Markov, E. Amsterdam, P. W. M. Blom, A. B. Sieval, and J. C. Hummelen, "Accurate measurement of the exciton diffusion length in a conjugated polymer using a heterostructure with a side-chain cross-linked fullerene layer," J. Phys. Chem. A **109**, 5266–5274 (2005).
[7]K. Kim and D. L. Carroll, "Roles of Au and Ag nanoparticles in efficiency enhancement of poly(3-octylthiophene)/C60 bulk heterojunction photovoltaic devices," Appl. Phys. Lett. **87**, 203113 (2005).
[8]K. L. Kelly, E. Coronado, L. L. Zhao, and G. C. Schatz, "The optical properties of metal naoparticles: The influence of size, shape, and dielectric enviroment," J. Phys. Chem. B **107**, 668–677 (2003).
[9]S. A. Maier, *Plasmonics: Fundamentals and Applications* (Springer, 2007).
[10]J. M. Montgomery, T.-W. Lee, and S. K. Gray, "Theory and modeling of light interactions with metallic nanostructures," J. Phys.: Condens. Matter **20**, 323201 (2008).
[11]M. Rycenga, C. M. Cobley, J. Zeng, W. Li, C. H. Moran, Q. Zhang, D. Qin, and Y. Xia, "Controlling the synthesis and assembly of silver nanostructrues for plasmonic applications," Chem. Rev. **111**, 3669–3712, (2011).
[12]M. A. Garcia, "Surface plasmons in metallic nanoparticles: Fundamentals and applications," J. Phys. D: Appl. Phys. **45**, 389501 (2012).
[13]X. Fan, W. Zheng, and D. J. Singh, "Light scattering and surface plasmons on small spherical particles," Light: Sci. Appl. **3**, e179 (2014).
[14]H. A. Atwater and A. Polman, "Plasmonics for improved photovoltaic devices," Nat. Mater. **9**, 205–213 (2010).
[15]B. P. Rand, P. Peumans, and S. R. Forrest, "Long-range absorption enhancement in organic tandem thin-film solar cells containing silver nanoclusters," J. Appl. Phys. **96**, 7519–7526 (2004).
[16]K. R. Catchpole and A. Polman, "Design principles for particle plasmon enhanced solar cells," Appl. Phys. Lett. **93**, 191113 (2008).
[17]H. Shen, P. Bienstman, and B. Maes, "Plasmonic absorption enhancement in organic solar cells with thin active layers," J. Appl. Phys. **106**, 073109 (2009).
[18]X. Chen, B. Jia, Y. Zhang, and M. Gu, "Exceeding the limit of plasmonic light trapping in textured screen-printed solar cells using Al nanoparticles and wrinkle-like graphene sheets," Light: Sci. Appl. **2**, e92 (2013).
[19]C. F. Guo, T. Sun, F. Cao, Q. Liu, and Z. Ren, "Metallic nanostructures for light trapping in energy-harvesting devices," Light: Sci. Appl. **3**, e161 (2014).
[20]P. Y. Silvert, R. H. Urbina, and K. T. Elhsissen, "Preparation of colloidal silver dispersions by the polyol process," J. Mater. Chem. **7**(2), 293–299, (1997).
[21]D. W. Lynch and W. R. Hunter, in *Handbook of Optical Constants of Solids*, edited by E. D. Palik (Academic, 1985), pp. 275–368.
[22]F. Monestier, J. J. Simon, P. Torchio, L. Escoubas, F. Flory, S. Bailly, R. Bettignies, S. Guillerez, and C. Defranoux, "Modeling the short-circuit current density of polymer solar cells based on P3HT:PCBM blend," Sol. Energy Mater. Sol. Cells **91**, 405–410 (2007).
[23]See supplementary material at http://dx.doi.org/10.1063/1.4898600 for figures of the field distribution (Figure S1), field enhancement (Figure S2), and field components (Figure S3) of Ag NSs arrays that embedded in P3HT.
[24]K. X. Wang, Z. Yu, V. Liu, Y. Cui, and S. Fan, "Absorption enhancement in ultrathin crystalline silicon solar cells with antireflection and light-trapping nanocone gratings," Nano Lett. **12**, 1616–1619 (2012).